Artificial Immune Systems Approach for Surface Reconstruction of Shapes with Large Smooth Bumps

Akemi Gálvez[1,2], Iztok Fister Jr.[3], Lihua You[4], Iztok Fister[3], and Andrés Iglesias[1,2†]

[1] Dept. of Applied Mathematics & Computational Sciences, University of Cantabria, 39005 Santander, Spain

[2] Faculty of Pharmaceutical Sciences, Toho University, 2-2-1 Miyama, 274-8510 Funabashi, Japan

{galveza,iglesias}@unican.es

[3] Faculty of Electrical Engineering and Computer Science, University of Maribor, Maribor, Slovenia

{iztok.fister1,iztok.fister}@um.si

[4] National Center for Computer Animation, Faculty of Media & Communication, Bournemouth University, Poole BH12 5BB, UK

lyou@bournemouth.ac.uk

[†]Corresponding author

Abstract. Reverse engineering is one of the classical approaches for quailty assessment in industrial manufacturing. A key technology in reverse engineering is surface reconstruction, which aims at obtaining a digital model of a physical object from a cloud of 3D data points obtained by scanning the object. In this paper we address the surface reconstruction problem for surfaces that can exhibit large smooth bumps. To account for this type of features, our approach is based on using exponentials of polynomial functions in two variables as the approximating functions. In particular, we consider three different models, given by bivariate distributions obtained by combining a normal univariate distribution with a normal, Gamma, and Weibull distribution, respectively. The resulting surfaces depend on some parameters whose values have to be optimized. This yields a difficult nonlinear continuous optimization problem solved through an artificial immune systems approach based on the clonal selection theory. The performance of the method is discussed through its application to a benchmark comprised of three examples of point clouds.

Keywords: Artificial intelligence, reverse engineering, surface reconstruction, artificial immune systems, bivariate distributions, point clouds, data fitting

1 Introduction

1.1 Motivation

Nowadays, there is a renewed and increasing interest in the fields of artificial intelligence (AI) and machine learning (ML). This popularity is due in large part

ICCS Camera Ready Version 2023
To cite this paper please use the final published version:
DOI: 10.1007/978-3-031-36027-5_22

to the extraordinary advances of AI and ML in areas such as pattern recognition, computer vision, robotics, healthcare, self-driving cars, natural language processing, automatic machine translation, and many others. The industrial sector is at the core of most of these innovations, with initiatives such as Industry 4.0, and Internet of Things (IoT), paving the way to a new field commonly known as *industrial artificial intelligence*. By this term we refer to the application of AI and ML methods and developments to industrial processes in order to improve the production and manufacturing systems.

One of the most interesting applications of industrial artificial intelligence arises in *quality assessment*, where typically AI methods are applied to analyze the quality of a digital design or a manufactured workpiece to determine whether or not certain aesthetic and/or functional objectives are met. In many industrial settings, quality assessment is carried out through *reverse engineering*, where the goal is to obtain a digital replica of a manufactured good. For instance, reverse engineering is widely used in the design and manufacturing of CAD models for car bodies in the automotive industry, plane fuselages for the aerospace industry, ship hulls in shipbuilding industry, moulds and lasts in footwear industry, components for home appliances, cases for consumer electronics, and in many other fields [32].

A key technology in reverse engineering is *surface reconstruction* [36]. Starting with a cloud of 3D data points obtained by 3D scanning of the physical object, surface reconstruction aims to recover the underlying shape of the real object in terms of mathematical equations of the surfaces fitting these data points, which is a much better way to store and manipulate the geometric information than using the discrete data points directly. These mathematical equations can then be efficiently used for different computer-assisted quality assessment processes, such as shape interrogation, shape analysis, failure detection and diagnosis, and many others. This approach is also used for intellectual property right assessment, industrial property plagiarism control, and other industrial and legal issues.

A central problem in surface reconstruction is the selection of the approximating functions. Classical choices are the free-form parametric polynomial surfaces, such as the Bézier and the B-spline surfaces, which are widely used in computer graphics and geometric design. However, it has been noticed that depending on the geometry of the point cloud, other choices might also be adequate. For instance, exponential functions are particularly suitable to model surfaces with large smooth bumps, as evidenced by the shape of the Gaussian function. Yet, it is difficult to manipulate shapes with a simple exponential function. The exponential of polynomial functions of two variables provides more flexibility, as it introduces extra degrees of freedom that can be efficiently used to modify the global shape of the surface while handling local features as well. Owing to these reasons, this is the approach followed in this paper.

1.2 Aims and structure of this paper

In this paper we address the problem of surface reconstruction from data points by using exponentials of polynomial functions in two variables as the approximat-

ICCS Camera Ready Version 2023
To cite this paper please use the final published version:
DOI: 10.1007/978-3-031-36027-5_22

ing functions. In particular, we consider three different models of exponentials of polynomial functions, given by bivariate distributions obtained by combining a normal univariate distribution with a normal, Gamma, and Weibull distribution, respectively. The resulting surfaces depend on some parameters whose values have to be optimized. This yields a difficult nonlinear continuous optimization problem that will be solved through an artificial immune systems approach called ClonalG. The performance of the method will be discussed through its application to a benchmark comprised of three examples of point clouds.

The structure of this paper is as follows: Sect. 2 summarizes the previous work in the field. Sect. 3 describes the optimization problem addressed in this work. Our method to solve it is described in detail in Sect. 4. The performance of the method is illustrated through three illustrative examples, which are discussed in Sect. 5. The paper closes in Sect. 6 with the main conclusions and some ideas for future work in the field.

2 Previous Work

The issue of surface reconstruction for shape quality assessment has been as topic of research for decades. Early computational algorithms were introduced the 60s and 70s, mostly based on numerical methods [11, 33, 34]. Subsequent advances during the 80s and 90s applied more sophisticated techniques, although they failed to provided general solutions [3, 10]. From a mathematical standpoint, this issue can be formulated as a least-squares optimization problem [26, 28, 31]. However, classical mathematical optimization techniques had little success in solving it beyond rather simple cases, so the scientific community focused on alternative approaches, such as error bounds [29], dominant points [30] or curvature-based squared distance minimization [37]. These methods provide acceptable results but they need to meet strong conditions such as high differentiability and noiseless data that are not so common in industrial settings.

More recently, methods based on artificial intelligence and soft computing are receiving increasing attention. Some approaches are based on neural networks [18], self-organizing maps [19], or the hybridization of neural networks with partial differential equations [2]. These neural approaches have been extended to functional networks in [20, 27] and hybridized with genetic algorithms [16]. Other approaches are based on support vector machines [25] and estimation of distribution algorithms [40]. Other techniques include genetic algorithms [17, 38, 39], particle swarm optimization [12, 13], firefly algorithm [14], cuckoo search algorithm [22, 24], artificial immune systems [23], and hybrid techniques [15, 21, 35]. It is important to remark that none of the previous approaches addressed the problem discussed in this paper.

3 The Optimization Problem

As explained above, our approach to the surface reconstruction problem is to consider exponential of bivariate polynomial functions as the fitting functions.

ICCS Camera Ready Version 2023
To cite this paper please use the final published version:
DOI: 10.1007/978-3-031-36027-5_22

A suitable way to proceed in this regards is to consider bivariate distributions whose conditionals belong to such families of basis functions [4, 5]. In particular, we consider the combination of a normal univariate distribution with the normal, Gamma, and Weibull distributions, respectively. In the first case, the approximating function takes the form:

$$f(x,y) = e^{\frac{C_0}{2} - C_2\,x + C_1\,\frac{x^2}{2} - C_3\,\frac{y^2}{2} - C_4\,\frac{x^2y^2}{2} + C_5xy^2 + C_6y + C_7x^2y - 2C_8xy} \tag{1}$$

which is a model depending on 9 parameters. However, these parameters are not fully free, as they have to fulfill some constraints such as non-negativity and integrability, leading to the following constraints (see [1] for details):

$$C_4 > 0 \quad ; \quad C_3C_4 > C_5^2 \quad ; \quad -C_1C_4 > C_7^2 \tag{2}$$

In the second case, the approximating function is given by:

$$f(x,y) = e^{F + Ay - Cy^2 + (G + By - Dy^2)x + (H + Jy - Ky^2)log(x)} \tag{3}$$

which depends on 9 parameters, with the constraints:

$$C > 0 \quad ; \quad D > 0 \quad ; \quad G < \frac{-B^2}{4D} \quad ; \quad H > -1 \quad ; \quad J = 0 \quad ; \quad K = 0 \tag{4}$$

The third model is given by:

$$f(x,y) = e^{D + L\,x + F\,x^2 - \left(A + B\,x + G\,x^2\right)(y-K)^C} \; (y - K)^{C-1} \tag{5}$$

which is a model depending on 8 parameters with the following constraints:

$$G \geqslant 0 \quad ; \quad 4GA \geqslant B^2 \quad ; \quad C > 0 \quad ; \quad F < 0 \tag{6}$$

Once the approximating function is selected, the surface reconstruction procedure requires to compute the parameters of the function to obtain an accurate mathematical representation of the function $f(x,y)$ approximating the point cloud accurately. This condition can be formulated as the minimization problem:

$$min \left\{ \sum_{p=1}^{P} \left[(x_p - \hat{x_p})^2 + (y_p - \hat{y_p})^2 + (z_p - f(\hat{x_p}, \hat{y_p}))^2 \right] \right\} \tag{7}$$

where (x_p, y_p, z_p) and $(\hat{x_p}, \hat{y_p}, \hat{z_p})$ denote the original and reconstructed data points, respectively, and $\hat{x_p}$ and $\hat{y_p}$ can be obtained by projecting the point cloud onto a flat surface $B(x,y)$ determined by principal component analysis. Also, our minimization problem is restricted to the support of the function $f(x,y) - B(x,y)$ and subjected to some parametric constraints given by the pairs of Eqs. (1)-(2), Eqs. (3)-(4), and Eqs. (5)-(6), respectively.

This minimization problem is very difficult to solve, as it becomes a constrained, multivariate, nonlinear, multimodal continuous optimization problem. As a consequence, usual gradient-based mathematical techniques are not suitable to solve it. In this paper, we apply a powerful artificial immune systems algorithm called ClonalG to solve this problem. It is explained in detail in next section.

ICCS Camera Ready Version 2023
To cite this paper please use the final published version:
DOI: 10.1007/978-3-031-36027-5_22

4 The Proposed Method: ClonalG Algorithm

The *ClonalG algorithm* is a computational method of the family of artificial immune systems (AIS), which are nature-inspired metaheuristic methods based on different aspects and features of the natural immune systems of humans and other mammals [6, 7]. In particular, the ClonalG algorithm is based on the widely accepted clonal selection theory, used to explain how the immune system reacts to antigenic stimulus [8, 9]. When a new antigen Ag attacks the human body, our immune system elicits an immunological response in the form of antibodies Ab, which are initially only slightly specific to the antigen. A measure of the affinity between the antibodies and the antigen determines which antibodies will be selected for proliferation: those with the highest affinity with the antigen, with the rest being removed from the pool. The selected antibodies undergo an affinity maturation process that enhances their affinity to the antigen over the time. A somatic mutation on the selected antibodies promotes higher diversity of the population of antibodies, so that the affinity improves further during the process. This mutation process is carried out at a much higher (about five or six orders of magnitude) rate than normal mutation, and is therefore called somatic hypermutation.

The ClonalG method was originally envisioned for pattern recognition tasks, using this natural process of immune response as a metaphor. The patterns to be learned (or input patterns) play the role of antigens, which are presented to the computational system (a metaphor of the human body). Whenever a pattern A is to be recognized, it is presented to a population of antibodies B_i, and the affinity between the couples (A, B_i) is computed based on a measure of the pattern similarity (for instance, the Hamming distance between images).

The algorithm is population-based, as it maintains a population of antibodies representing the potential matching patterns, and proceeds iteratively, along generations. It is summarized as follows (see [8, 9] for further details):

1. An antigen Ag_j is randomly selected and presented to the collection of antibodies Ab_i, with $i = 1, \dots, M$, where M is the size of the set of antibodies.
2. A vector affinity $\mathbf{f}$ is computed, as $f_i = Af(Ab_i, Ag_j)$ where Af represents the affinity function.
3. The N highest affinity components of $\mathbf{f}$ are selected for next step.
4. The selected antibodies are cloned adaptively, with the number of clones proportional to the affinity.
5. The clones from the previous step undergo somatic hypermutation, with the maturation rate inversely proportional to the affinity.
6. A new vector affinity **f'** on the new matured clones is computed.
7. The highest affinity antibodies from set of matured clones are selected for a memory pool. This mechanism is intended as an elitist strategy to preserve the best individuals for next generations.
8. The antibodies with the lowest affinity are replaced by new random individuals and inserted into the whole population along with the memory antibodies.

ICCS Camera Ready Version 2023
To cite this paper please use the final published version:
DOI: 10.1007/978-3-031-36027-5_22

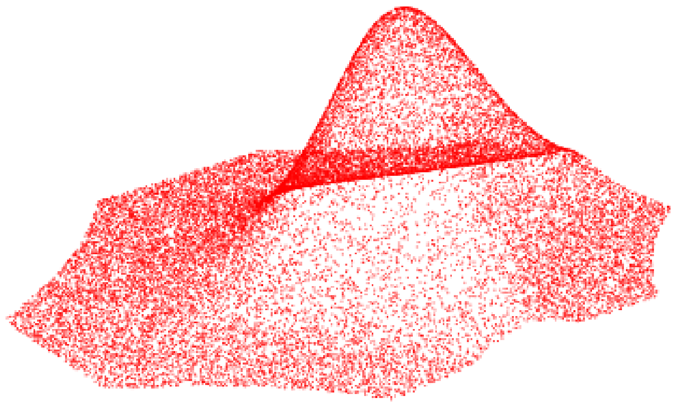

Fig. 1. Original point cloud of *Example I*.

The algorithm is repeated for a given number of generations, N_{gen}, which is a parameter of the method. This algorithm has proved to be efficient for pattern recognition tasks. With some modifications, it can also be applied to solve optimization problems. In short, the main modification is that, for optimization problems, there is no pattern to be learned; instead, a fitness function has to be optimized. In that case, the whole population can be cloned, although it is convenient to preserve an unmuted copy of the best individuals during the maturation step to speed up the method convergence.

Regarding the parameter tuning of the method, the only parameters of the ClonalG algorithm are the population size and the maximum number of iterations. We applied a fully empirical approach for the choice of these values: they have been determined after conducting several computer simulations for different parameter values. After this step, we selected a population of 50 individuals (antibodies) for the method, and a total number of 500 iterations, which have been more than enough to reach convergence in all our simulations. The best solution reached at the final iteration is selected as the optimal solution of the minimization problem in this work.

5 Experimental Results

The method described in the previous section has been applied to several examples of point clouds. For limitations of space, we restrict our discussion to three illustrative examples, fitted according to the models in Eqs. (1), (3), and (5) for *Example I*, *Example II*, and *Example III*, respectively, as discussed in the following paragraphs.

ICCS Camera Ready Version 2023
To cite this paper please use the final published version:
DOI: 10.1007/978-3-031-36027-5_22

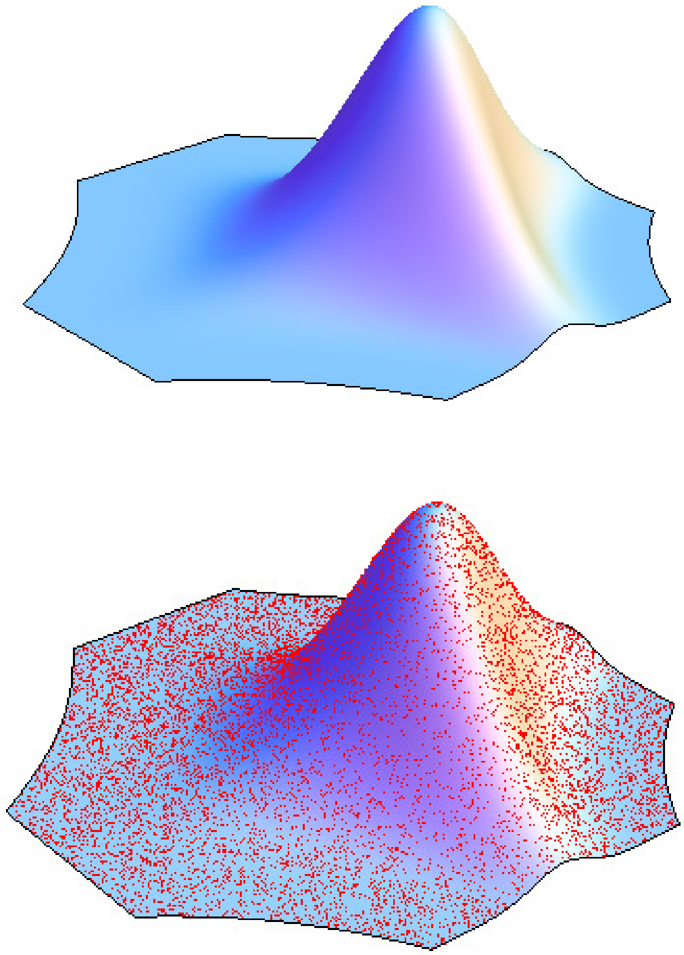

Fig. 2. *Example I*: (top) Reconstructed surface; (bottom) reconstructed surface and data points.

5.1 Example I

This example consists of a cloud of $R = 32,167$ three-dimensional data points displayed in Fig. 1. The data points do not follow a uniform parameterization and are affected by white noise of low intensity (SNR=10). The point cloud is fitted with model 1 according to Eq. (1) with the constraints in Eq. (2). Therefore, the resulting optimization problem consists of minimizing the functional:

ICCS Camera Ready Version 2023
To cite this paper please use the final published version:
DOI: 10.1007/978-3-031-36027-5_22

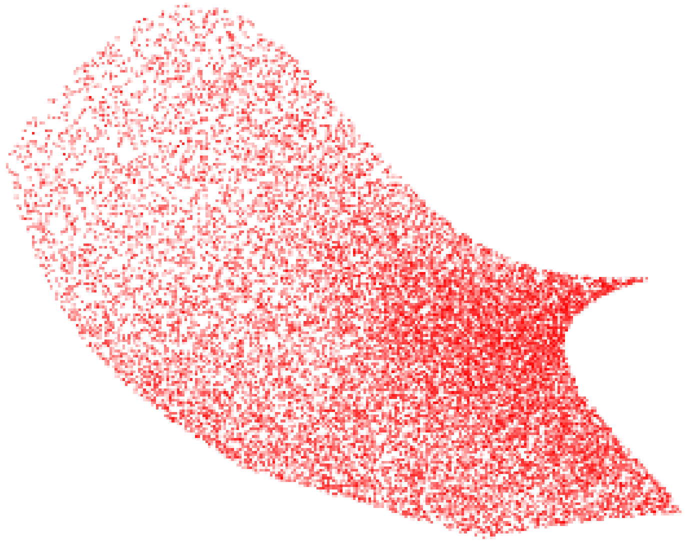

Fig. 3. Original point cloud of *Example II*.

$$\Xi = \sum_{p=1}^{P} \left[(x_p - \hat{x_p})^2 + (y_p - \hat{y_p})^2 + (z_p - f(\hat{x_p}, \hat{y_p}))^2 \right]$$

for

$$f(\hat{x_p}, \hat{y_p}) = e^{\frac{C_0}{2} - C_2\, \hat{x_p} + C_1\, \frac{\hat{x_p}^2}{2} - C_3\, \frac{\hat{y_p}^2}{2} - C_4\, \frac{\hat{x_p}^2 \hat{y_p}^2}{2} + C_5 \hat{x_p} \hat{y_p}^2 + C_6 y + C_7 \hat{x_p}^2 \hat{y_p} - 2C_8 \hat{x_p} \hat{y_p}}$$

Applying our method to the minimization of the functional Ξ with the constraints in Eq. (2) we obtained the values: $C_0 = -3.1815; C_1 = -0.9936; C_2 = -0.8977; C_3 = 1.0249; C_4 = 0.9892; C_5 = 0.0073; C_6 = 0.9105; C_7 = 0.0104; C_8 = 0.0027$. For these values, the mean squared error (MSE), denoted in this paper as Δ and defined as $\Delta = \frac{\Xi}{P}$, becomes: $\Delta = 0.02417$, which shows that the method is pretty accurate in recovering the underlying shape of data.

The best reconstructed surface is displayed in Fig. 2(top), where the bottom picture shows the superposition of the fitting surface and the original point cloud for better visualization. From that figure, the good numerical accuracy of the method is visually confirmed, as the fitting surface reproduces the global shape of the point cloud with very good visual fidelity. Note also that the shape of the prominent bump at the center of the surface is faithfully reconstructed.

ICCS Camera Ready Version 2023
To cite this paper please use the final published version:
DOI: 10.1007/978-3-031-36027-5_22

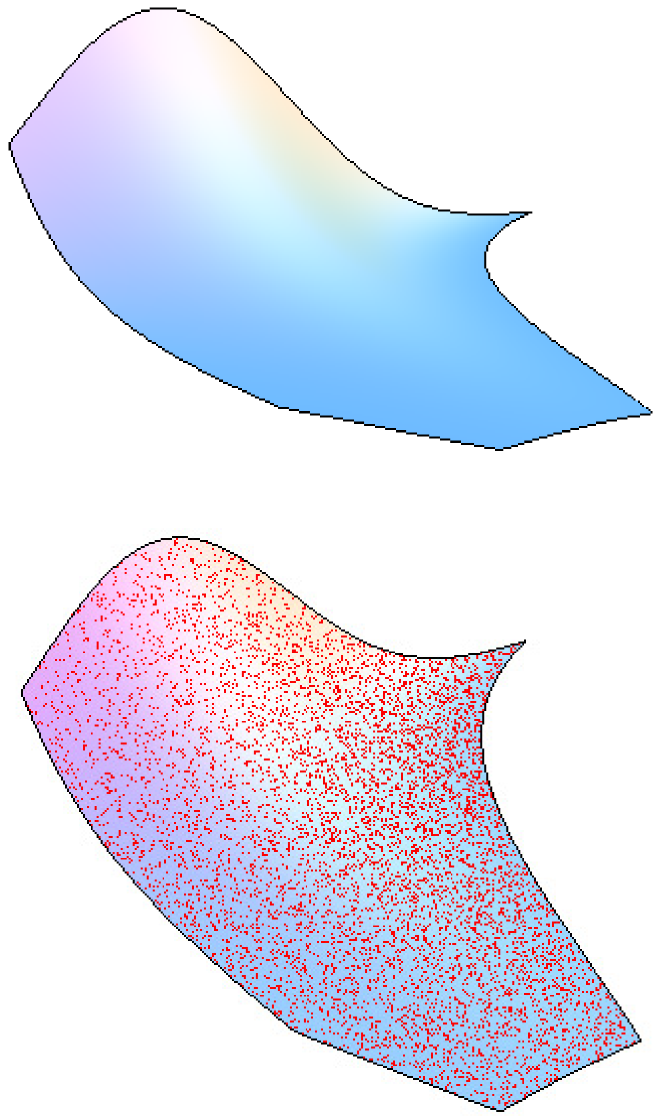

Fig. 4. *Example II*: (top) Reconstructed surface; (bottom) reconstructed surface and data points.

5.2 Example II

The second example consists of a cloud of $R = 30,753$ three-dimensional data points shown in Fig. 3. The point cloud is fitted with model 2 according to Eq. (3)

ICCS Camera Ready Version 2023
To cite this paper please use the final published version:
DOI: 10.1007/978-3-031-36027-5_22

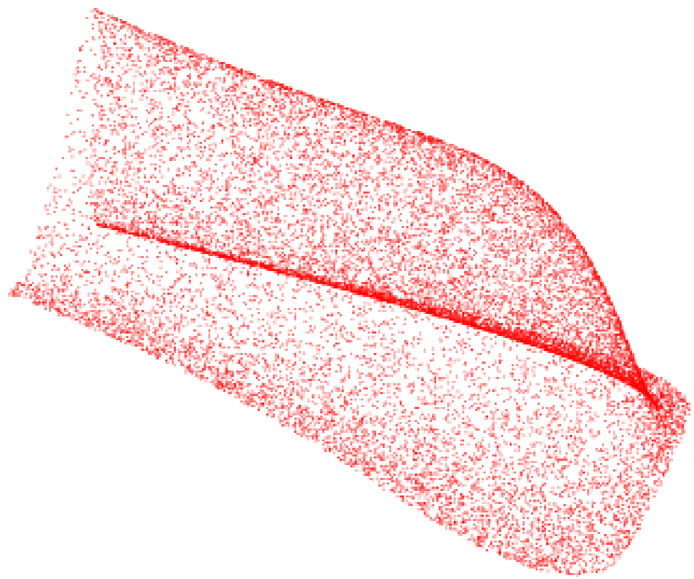

Fig. 5. Original point cloud of *Example III*.

with the constraints in Eq. (4). Application of the ClonalG method described in Sect. 4 yields the values: $A = 2.9782; B = 2.0273; C = 4.0792; D = 2.9885; K = 0.0; F = 3.9811; G = -1.0337; H = 0.0101; J = 0.0$, for which the mean squared error takes the value: $\Delta = 0.01352$, an excellent indicator of good fitting. Note also that $J = K = 0$ is not directly obtained from the optimization method but given as an input to the method via the constraints in Eq. (4).

Fig. 4 shows the optimal reconstructed surface (top) and its superposition with the point cloud (bottom). Note again the excellent visual quality of the surface reconstruction from the point cloud in Fig. 3, which confirms our good numerical results.

5.3 Example III

For the third example, we consider the cloud point depicted in Fig. 5. In this case, the point cloud consists of $R = 30,679$ data points, which is fitted according to Eq. (5) with the constraints in Eq. (6).

Application of our method yields the values: $A = 2.0204; B = -3.9926; C = 1.9905; D = 3.0168; L = 0.0116; F = -2.0068; G = 1.9851; K = 0.0104$, for which the mean squared error takes the value: $\Delta = 0.09212$, which is considered a satisfactory approximation. The resulting best approximating surface is shown in Fig. 6 (top) and superimposed by the original point cloud in Fig. 6 (bottom).

ICCS Camera Ready Version 2023
To cite this paper please use the final published version:
DOI: 10.1007/978-3-031-36027-5_22

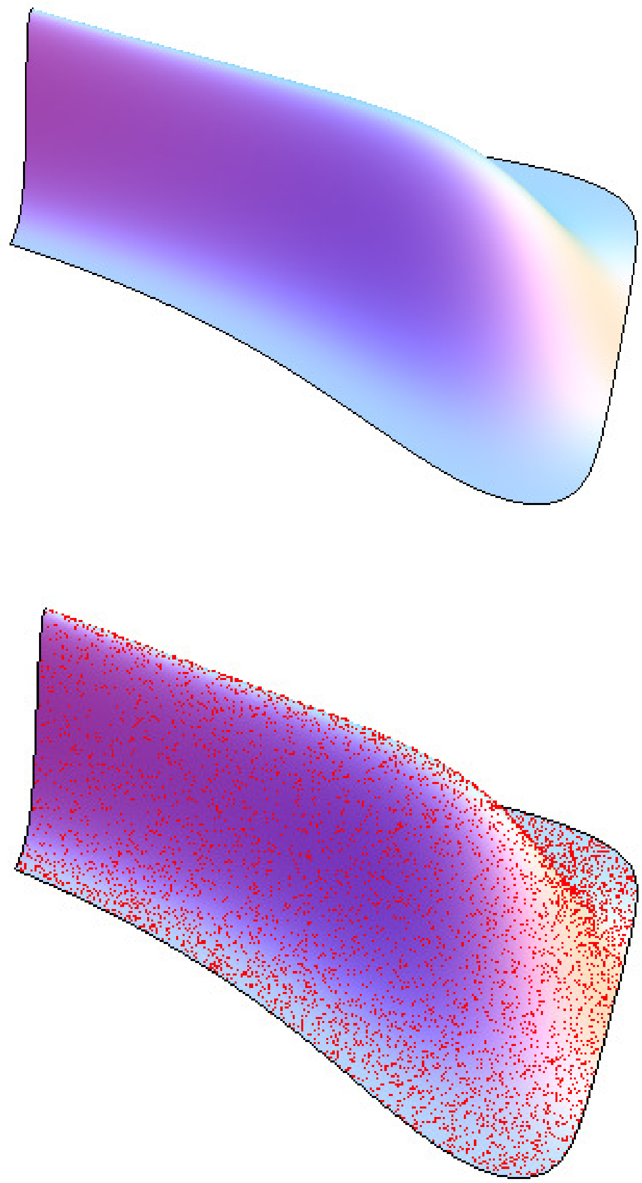

Fig. 6. *Example III*: (top) Reconstructed surface; (bottom) reconstructed surface and data points.

ICCS Camera Ready Version 2023
To cite this paper please use the final published version:
DOI: 10.1007/978-3-031-36027-5_22

Once again,we remark that the large surface bump at the center is accurately reconstructed.

5.4 Implementation issues

The computations in this paper have been carried out on a PC desktop with a processor Intel Core i9 running at 3.7 GHz and with 64 GB of RAM. The source code has been implemented by the authors in the programming language of the scientific program *Mathematica* version 12. About the computational times, our method is quite fast. Each execution of the method takes only a few seconds of CPU time, depending on the population size, number of iterations, complexity of the problem, and other factors. For reference, the executions of the examples in this paper take about 3–6 seconds.

6 Conclusions and Future Work

This paper addresses the surface reconstruction problem from 3D point clouds for surfaces that can exhibit large smooth bumps. To account for this type of features, our approach is based on using exponentials of polynomial functions in two variables as the approximating functions. Three different models, given by bivariate distributions obtained by combining a normal univariate distribution with a normal, Gamma, and Weibull distribution, are considered as fitting functions. Each model leads to surfaces depending on some parameters whose values have to be optimized. However, this yields a difficult nonlinear continuous optimization problem that cannot be solved by traditional numerical optimization techniques. To overcome this limitation, we apply an artificial immune systems approach called ClonalG, which is based on the clonal selection theory. The performance of the method is discussed through its application to a benchmark comprised of three examples of point clouds. The computational results show that the method obtains good visual and numerical results, and is able to reconstruct the subtle bump features of the underlying shape of data with good accuracy.

Regarding the future work in the field, we want to extend this method to other families of surfaces exhibiting different types of features, such as holes, critical points, discontinuities, and the like. We also want to apply this methodology to complex workpieces from manufacturing industries that can typically require to satisfy other types of functional and/or design constraints. The consideration of other metaheuristic techniques to solve the optimization problem more efficiently and the comparison of our results with other state-of-the-art methods described in the literature are also part of our plans for future work in the field.

Acknowledgment

Akemi Gálvez, Lihua You and Andrés Iglesias thank the financial support from the project PDE-GIR of the European Union's Horizon 2020 research and innovation programme, in the Marie Sklodowska-Curie Actions programme, with grant agreement of reference number 778035, and also from the Agencia Estatal de Investigación (AEI) of the Spanish Ministry of Science and Innovation (Computer Science National Program), for the grant of reference number PID2021-127073OB-I00 of the MCIN/AEI/10.13039/501100011033/FEDER, EU. Iztok Fister Jr. thanks the Slovenian Research Agency for the financial support under Research Core Funding No. P2-0057. Iztok Fister thanks the Slovenian Research Agency for the financial support under Research Core Funding No. P2-0042 - Digital twin.

References

1. Arnold, B., Castillo, E., Sarabia, J.M.: *Conditionally Specified Distributions*. Springer Verlag, Lecture Notes in Statistics, **73**, Berlin, Germany (1992).
2. Barhak, J., Fischer, A.: Parameterization and reconstruction from 3D scattered points based on neural network and PDE techniques. *IEEE Trans. on Visualization and Computer Graphics*, **7**(1) (2001) 1-16.
3. Barnhill, R.E.: *Geometric Processing for Design and Manufacturing*. SIAM, Philadelphia (1992).
4. Castillo, E., Iglesias, A.: Some characterizations of families of surfaces using functional equations. *ACM Transactions on Graphics*, **16**(3) (1997) 296-318.
5. Castillo, E., Iglesias, A., Ruiz, R.: *Functional Equations in Applied Sciences*. Elsevier Science, Mathematics in Science and Engineering, **199**, Amsterdam, The Netherlands (2004).
6. Dasgupta, D. (editor): *Artificial Immune Systems and Their Applications*. Springer Verlag, Berlin (1999).
7. De Castro, L.N., Timmis, J.: *Artificial Immune Systems: A New Computational Intelligence Approach*. Springer-Verlag, London (2002).
8. De Castro, L.N., Von Zuben, F.J.: *Artificial Immune Systems: Part I - Basic Theory and Applications*, Technical Report-RT DCA 01/99 (1999).
9. De Castro, L.N., Von Zuben, F.J.: Learning and optimization using the clonal selection principle. *IEEE Transactions on Evolutionary Computation*, **6**(3) (2002) 239-251.
10. Dierckx, P.: *Curve and Surface Fitting with Splines*. Oxford University Press, Oxford (1993).
11. Farin, G.: *Curves and surfaces for CAGD (5th ed.)*. Morgan Kaufmann, San Francisco (2002).
12. Gálvez, A., Iglesias A.: Efficient particle swarm optimization approach for data fitting with free knot B-splines. *Computer-Aided Design*, **43**(12) (2011) 1683-1692.
13. Gálvez A., Iglesias A.: Particle swarm optimization for non-uniform rational B-spline surface reconstruction from clouds of 3D data points. *Information Sciences*, **192**(1) (2012) 174-192.
14. Gálvez A., Iglesias A.: Firefly algorithm for polynomial Bézier surface parameterization. *Journal of Applied Mathematics*, **2013** Article ID 237984 (2012).
15. Gálvez A., Iglesias A.: A new iterative mutually-coupled hybrid GA-PSO approach for curve fitting in manufacturing. *Applied Soft Computing*, **13**(3) (2013) 1491-1504.
16. Gálvez, A., Iglesias, A., Cobo, A., Puig-Pey, J., Espinola, J.: Bézier curve and surface fitting of 3D point clouds through genetic algorithms, functional networks and least-squares approximation. *Lectures Notes in Computer Science*, **4706** (2007) 680-693.

ICCS Camera Ready Version 2023
To cite this paper please use the final published version:
DOI: 10.1007/978-3-031-36027-5_22

17. Gálvez, A., Iglesias A., Puig-Pey J.: Iterative two-step genetic-algorithm method for efficient polynomial B-spline surface reconstruction. *Information Sciences*, **182**(1) (2012) 56-76.
18. Gu, P., Yan, X.: Neural network approach to the reconstruction of free-form surfaces for reverse engineering. *Computer-Aided Design* **27**(1) (1995) 59-64.
19. Hoffmann, M.: Numerical control of Kohonen neural network for scattered data approximation. *Numerical Algorithms*, **39**, (2005) 175-186.
20. Iglesias, A., Echevarría, G., Gálvez, A.: Functional networks for B-spline surface reconstruction. *Future Generation Computer Systems*, **20**(8) (2004) 1337-1353.
21. Iglesias, A., Gálvez, A.: Hybrid functional-neural approach for surface reconstruction. *Mathematical Problems in Engineering*, (2014) Article ID 351648, 13 pages.
22. Iglesias, A., Gálvez, A., Avila, A.: Hybridizing mesh adaptive search algorithm and artificial immune systems for discrete rational Bézier curve approximation. *The Visual Computer*, **32**, 393–402 (2016).
23. Iglesias, A., Gálvez, A., Avila, A.: Immunological approach for full NURBS reconstruction of outline curves from noisy data points in medical imaging. *IEEE/ACM Transactions on Computational Biology and Bioinformatics*, **15** (6), 929-1942 (2018).
24. Iglesias, A., Gálvez, A., Suarez, P., Shinya, M., Yoshida, N., Otero, C., Manchado, C. Gómez-Jauregui, V.: Cuckoo search algorithm with Lévy flights for global-support parametric surface approximation in reverse engineering. *Symmetry*, **10** (3), PaperID 58 (2018).
25. Jing, L., Sun, L.: Fitting B-spline curves by least squares support vector machines. In: *Proc. of the 2nd. Int. Conf. on Neural Networks & Brain*. Beijing (China). IEEE Press (2005) 905-909.
26. Jupp, D.L.B.: Approximation to data by splines with free knots. *SIAM Journal of Numerical Analysis*, **15** (1978) 328-343.
27. Knopf, G.K., Kofman, J.: Adaptive reconstruction of free-form surfaces using Bernstein basis function networks. *Engineering Applications of Artificial Intelligence*, **14**(5) (2001) 577-588.
28. Ma, W.Y., Kruth, J.P.: Parameterization of randomly measured points for least squares fitting of B-spline curves and surfaces. *Computer-Aided Design*, **27**(9) (1995) 663-675.
29. Park, H.: An error-bounded approximate method for representing planar curves in B-splines. *Computer Aided Geometric Design* **21** (2004) 479-497.
30. Park, H., Lee, J.H.: B-spline curve fitting based on adaptive curve refinement using dominant points. *Computer-Aided Design* **39** (2007) 439-451.
31. Patrikalakis, N.M., Maekawa, T.: *Shape Interrogation for Computer Aided Design and Manufacturing*. Springer Verlag, Heidelberg (2002).
32. Pottmann, H., Leopoldseder, S., Hofer, M., Steiner, T., Wang, W.: Industrial geometry: recent advances and applications in CAD. *Computer-Aided Design*, **37** (2005) 751-766.
33. Powell, M.J.D.: Curve fitting by splines in one variable. In: Hayes, J.G. (editor): *Numerical approximation to functions and data*. Athlone Press, London (1970).
34. Rice, J.R.: *The Approximation of Functions. Vol. 2*. Addison-Wesley, Reading, MA (1969).
35. Sarfraz, M., Raza, S.A.: Capturing outline of fonts using genetic algorithms and splines. *Proc. of Fifth International Conference on Information Visualization IV'2001*, IEEE Computer Society Press (2001) 738-743.
36. Varady, T., Martin, R.: Reverse Engineering. In: Farin, G., Hoschek, J., Kim, M. (eds.): *Handbook of Computer Aided Geometric Design*. Elsevier Science (2002).

ICCS Camera Ready Version 2023
To cite this paper please use the final published version:
DOI: 10.1007/978-3-031-36027-5_22

37. Wang, W.P., Pottmann, H., Liu, Y.: Fitting B-spline curves to point clouds by curvature-based squared distance minimization. *ACM Transactions on Graphics*, **25**(2) (2006) 214-238.
38. Yoshimoto, F., Moriyama, M., Harada, T.: Automatic knot adjustment by a genetic algorithm for data fitting with a spline. *Proc. of Shape Modeling International'99*, IEEE Computer Society Press (1999) 162-169.
39. Yoshimoto, F., Harada T., Yoshimoto, Y.: Data fitting with a spline using a real-coded algorithm. *Computer-Aided Design*, **35** (2003) 751-760.
40. Zhao, X., Zhang, C., Yang, B., Li, P.: Adaptive knot adjustment using a GMM-based continuous optimization algorithm in B-spline curve approximation. *Computer-Aided Design*, **43** (2011) 598-604.

ICCS Camera Ready Version 2023
To cite this paper please use the final published version:
DOI: 10.1007/978-3-031-36027-5_22